arXiv:1411.3100v2 [hep-ph] 17 Mar 2015

Semileptonic $B_s \to D_{s2}^*(2573)\ell\bar{\nu}_\ell$ transition in QCD

K. Azizi[1] *, H. Sundu[2] †, S. Şahin[2] ‡

[1] Department of Physics, Doğuş University, Acıbadem-Kadıköy, 34722 Istanbul, Turkey

[2] Department of Physics , Kocaeli University, 41380 Izmit, Turkey

Abstract

We analyze the semileptonic $B_s \to D_{s2}^*(2573)\ell\bar{\nu}_\ell$ transition, where $\ell = \tau,\ \mu$ or e, within the standard model. We apply the QCD sum rule approach to calculate the transition form factors entering the low energy Hamiltonian defining this channel. The fit functions of the form factors are used to estimate the total decay widths and branching fractions in all lepton channels. The orders of branching ratios indicate that this transition is accessible at LHCb in near future.

PACS number(s): 13.20.-v, 13.20.He, 11.55.Hx

*e-mail: kazizi@dogus.edu.tr

†e-mail: hayriye.sundu@kocaeli.edu.tr

‡e-mail: 095131004@kocaeli.edu.tr

1 Introduction

The semileptonic B meson decay channels are known as useful tools to accurately calculate the Standard Model (SM) parameters like determination of the Cabibbo-Kobayashi-Maskawa (CKM) quark mixing matrix, check the validity of the SM, describe the origin of the CP violation and search for new physics effects. By recent experimental progresses, it has become precise measurements available, and it is possible to perform precision calculations. Although the B meson decays are studied efficiently both theoretically and experimentally (see for instance [1–11]), most of B_s properties are not very clear yet (for some related theoretical and experimental studies on this meson see [12–21] and references therein). Since the detection and identification of this heavy meson is relatively difficult in the experiment, the theoretical and phenomenological studies on the spectroscopy and decay properties of this mesons can play essential role in our understanding of its non-perturbative dynamics, calculating the related parameters of the SM and providing opportunities to search for possible new physics contributions.

In the literature, there are a lot of theoretical studies devoted to the semileptonic transition of B_s into the pseudoscalar D_s and vector D_s^* charmed-strange mesons. But, we have no study on the semileptonic transitions of this meson into the tensor charmed-strange meson in final state, although it is expected to have considerable contribution to the total decay width of the B_s meson. In this accordance, in the present study, we investigate the semileptonic $B_s \to D_{s2}^*(2573)\ell\bar{\nu}_\ell$ transition in the framework of three-point QCD sum rule [22] as one of the most attractive and powerful techniques in hadron phenomenology, where the $D_{s2}^*(2573)$ is the low lying charmed-strange tensor meson with $J^P = 2^+$. In particular, we calculate the transition form factors entering the low energy matrix elements defining the transition under consideration. We find the working regions of the auxiliary parameters entering the calculations from different transformations, considering the criteria of the method used. This is followed by finding the behavior of the form factors in terms of the transferred momentum squared, which are then used to estimate the total width and branching fraction in all lepton channels. Note that the semileptonic $B \to D_2^*(2460)\ell\bar{\nu}_\ell$ decay channel is analyzed in [23] using the same method. The spectroscopic properties of the charmed-strange tensor meson $D_{s2}^*(2573)$ is also investigated in [24] using a two-point correlation function.

The layout of the paper is as follows. In next section, the QCD sum rules for the four form factors relevant to the semileptonic $B_s \to D_{s2}^*(2573)\ell\bar{\nu}_\ell$ transition are obtained. Section 3 contains numerical analysis of the form factors, calculation of their behavior in terms of q^2 as well as the estimation of the total decay width and branching ratio for the transition under consideration.

2 Theoretical framework

In order to calculate the form factors, associated with the semileptonic $B_s \to D_{s2}^*(2573)\ell\bar{\nu}_\ell$ transition via QCD sum rule formalism, we consider the following three-point correlation function:

$$\Pi_{\mu\alpha\beta} = i^2 \int d^4x \int d^4y e^{-ip.x} e^{ip'.y} \langle 0 \mid \mathcal{T}\Big[J^{D^*_{s2}(2573)}_{\alpha\beta}(y) J^{tr}_{\mu}(0) J^{B^\dagger_s}(x)\Big] \mid 0\rangle, \tag{1}$$

where $\mathcal{T}$ is the time ordering operator and $J^{tr}_{\mu}(0) = \bar{c}(0)\gamma_\mu(1-\gamma_5)b(0)$ is the transition current. The interpolating currents of the B_s and $D^*_{s2}(2573)$ mesons can be written in terms of the quark fields as

$$J^{B_s} = \bar{s}(x)\gamma_5 b(x), \tag{2}$$

and

$$J^{D^*_{s2}(2573)}_{\alpha\beta}(y) = \frac{i}{2}\Big[\bar{s}(y)\gamma_\alpha \overset{\leftrightarrow}{\mathcal{D}}_\beta(y) c(y) + \bar{s}(y)\gamma_\beta \overset{\leftrightarrow}{\mathcal{D}}_\alpha(y) c(y)\Big]. \tag{3}$$

Here $\overset{\leftrightarrow}{\mathcal{D}}_\beta(y)$ is the covariant derivative that acts on the left and right, simultaneously. It is given as

$$\overset{\leftrightarrow}{\mathcal{D}}_\beta(y) = \frac{1}{2}\Big[\overrightarrow{\mathcal{D}}_\beta(y) - \overleftarrow{\mathcal{D}}_\beta(y)\Big], \tag{4}$$

with

$$\begin{aligned}
\overrightarrow{\mathcal{D}}_\beta(y) &= \overrightarrow{\partial}_\beta(y) - i\frac{g}{2}\lambda^a A^a_\beta(y), \\
\overleftarrow{\mathcal{D}}_\beta(y) &= \overleftarrow{\partial}_\beta(y) + i\frac{g}{2}\lambda^a A^a_\beta(y),
\end{aligned} \tag{5}$$

where λ^a and $A^a_\beta(x)$ denote the Gell-Mann matrices and the external gluon fields, respectively.

According to the method used, in order to find the QCD sum rules for transition form factors, we shall calculate the aforesaid correlation function, once in terms of hadronic parameters and the second in terms of QCD parameters making use of operator product expansion (OPE). By equating these two representations to each other through a dispersion relation, we obtain the sum rules for form factors. To stamp down the contributions of the higher states and continuum, a double Borel transformation with respect to the p^2 and p'^2 is performed on both sides of the sum rules obtained and the quark-hadron duality assumption is used.

2.1 The hadronic representation

In order to calculate the hadronic side of the correlator in Eq.(1), we insert two complete sets of the initial B_s and the final $D^*_{s2}(2573)$ states with the same quantum numbers as the interpolating currents into the correlator. After performing four-integrals over x and y, we obtain

$$\begin{aligned}
\Pi^{had}_{\mu\alpha\beta} &= \frac{\langle 0 \mid J^{D^*_{s2}(2573)}_{\alpha\beta} \mid D^*_{s2}(2573)(p',\epsilon)\rangle \langle D^*_{s2}(2573)(p',\epsilon) \mid J^{tr}_{\mu}(0) \mid B_s(p)\rangle \langle B_s(p) \mid J^\dagger_{B_s} \mid 0\rangle}{(p^2 - m^2_{B_s})(p'^2 - m^2_{D^*_{s2}(2573)})} \\
&+ \cdots,
\end{aligned} \tag{6}$$

where $\cdots$ represents contributions of the higher states and continuum, and ϵ is the polarization tensor of the $D^*_{s2}(2573)$ tensor meson. We can parameterize the matrix elements appearing in the above equation in terms of decay constants, masses and form factors as

$$\begin{aligned}
\langle 0 \mid J^{D^*_{s2}(2573)}_{\alpha\beta} \mid D^*_{s2}(2573)(p',\epsilon)\rangle &= m^3_{D^*_{s2}(2573)} f_{D^*_{s2}(2573)} \epsilon_{\alpha\beta}, \\
\langle B_s(p) \mid J^{\dagger}_{B_s} \mid 0\rangle &= -i\frac{f_{B_s} m^2_{B_s}}{m_s + m_b}, \\
\langle D^*_{s2}(2573)(p',\epsilon) \mid J^{tr}_{\mu}(0) \mid B_s(p)\rangle &= h(q^2)\varepsilon_{\mu\nu\alpha\beta}\epsilon^{*\nu\lambda} P^{\lambda} P_{\alpha} q^{\beta} - iK(q^2)\epsilon^{*\mu\nu} P^{\nu} \\
&- i\epsilon^{*\alpha\beta} P^{\alpha} P^{\beta} \left[P_{\mu} b_+(q^2) + q_{\mu} b_-(q^2)\right], \qquad (7)
\end{aligned}$$

where $q = p - p'$, $P = p + p'$; and $h(q^2)$, $K(q^2)$, $b_+(q^2)$ and $b_-(q^2)$ are transition form factors. Now, we combine Eqs. (6) and (7) and performing summation over the polarization tensors via

$$\epsilon_{\alpha\beta}\epsilon^*_{\nu\theta} = \frac{1}{2} T_{\alpha\nu} T_{\beta\theta} + \frac{1}{2} T_{\alpha\theta} T_{\beta\nu} - \frac{1}{3} T_{\alpha\beta} T_{\nu\theta}, \qquad (8)$$

where

$$T_{\alpha\nu} = -g_{\alpha\nu} + \frac{p'_{\alpha} p'_{\nu}}{m^2_{D^*_{s2}(2573)}}. \qquad (9)$$

This procedure brings us to the final representation of the hadronic side, viz.

$$\begin{aligned}
\Pi^{had}_{\mu\alpha\beta} &= \frac{f_{D^*_{s2}} f_{B_s} m_{D^*_{s2}} m^2_{B_s}}{8(m_b + m_s)(p^2 - m^2_{B_s})(p'^2 - m^2_{D^*_{s2}})} \Bigg\{ \frac{2}{3}\Big[- \Delta K(q^2) + \Delta' b_-(q^2)\Big] q_{\mu} g_{\beta\alpha} \\
&+ \frac{2}{3}\Big[(\Delta - 4m^2_{D^*_{s2}}) K(q^2) + \Delta' b_+(q^2)\Big] P_{\mu} g_{\beta\alpha} + i(\Delta - 4m^2_{D^*_{s2}}) h(q^2) \varepsilon_{\lambda\nu\beta\mu} P_{\lambda} P_{\alpha} q_{\nu} \\
&+ \Delta K(q^2) q_{\alpha} g_{\beta\mu} + \text{other structures} \Bigg\} + ..., \qquad (10)
\end{aligned}$$

where

$$\Delta = m^2_{B_s} + 3m^2_{D^*_{s2}} - q^2, \qquad (11)$$

and

$$\Delta' = m^4_{B_s} - 2m^2_{B_s}(m^2_{D^*_{s2}} + q^2) + (m^2_{D^*_{s2}} - q^2)^2. \qquad (12)$$

2.2 The OPE representation

The OPE side of the correlation function is calculated in deep Euclidean region. For this aim, we insert the explicit forms of the interpolating currents into the correlation function in Eq. (1). After performing contractions via the Wick's theorem, we obtain the following result in terms of the heavy and light quarks propagators:

$$\begin{aligned}
\Pi^{OPE}_{\mu\alpha\beta} &= \frac{-i^3}{2} \int d^4x \int d^4y e^{-ip\cdot x} e^{ip'\cdot y} \\
&\times \Big\{ Tr\left[S^{ki}_s(x-y)\gamma_{\alpha} \overleftrightarrow{\mathcal{D}}_{\beta}(y) S^{ij}_c(y) \gamma_{\mu}(1-\gamma_5) S_b(-x)^{jk} \gamma_5 \right] + [\beta \leftrightarrow \alpha] \Big\}. \qquad (13)
\end{aligned}$$

The heavy and light quarks propagators appearing in above equation and up to terms taken into account in the calculations are given by

$$S_Q^{i\ell}(x) = \frac{i}{(2\pi)^4}\int d^4k e^{-ik\cdot x}\left\{\frac{\delta_{i\ell}}{\not k - m_Q} - \frac{g_s G_{i\ell}^{\alpha\beta}}{4}\frac{\sigma_{\alpha\beta}(\not k + m_Q) + (\not k + m_Q)\sigma_{\alpha\beta}}{(k^2-m_Q^2)^2} + \delta_{i\ell}\frac{\pi^2}{3}\langle\frac{\alpha_s GG}{\pi}\rangle\frac{m_Q k^2 + m_Q^2\not k}{(k^2-m_Q^2)^4} + \cdots\right\}, \quad (14)$$

where $Q = b$ or c, and

$$S_s^{ij}(x) = i\frac{\not x}{2\pi^2x^4}\delta_{ij} - \frac{m_s}{4\pi^2x^2}\delta_{ij} - \frac{\langle\bar s s\rangle}{12}\Big(1 - i\frac{m_s}{4}\not x\Big)\delta_{ij} - \frac{x^2}{192}m_0^2\langle\bar s s\rangle\Big(1 - i\frac{m_s}{6}\not x\Big)\delta_{ij} - \frac{ig_s G_{\theta\eta}^{ij}}{32\pi^2x^2}[\not x\sigma^{\theta\eta} + \sigma^{\theta\eta}\not x] + \cdots. \quad (15)$$

To proceed, we insert the expressions of the heavy and light propagators into Eq. (13) and perform the derivatives with respect to x and y. Then, we transform the calculations to the momentum space and make the $x_\mu \to i\frac{\partial}{\partial p_\mu}$ and $y_\mu \to -i\frac{\partial}{\partial p'_\mu}$ replacements. We perform the two four-integrals coming from the heavy quark propagators with the help of two Dirac delta functions appearing in the calculations. Finally, we perform the last four-integral using the Feynman parametrization, viz.

$$\int d^4t\frac{(t^2)^\beta}{(t^2+L)^\alpha} = \frac{i\pi^2(-1)^{\beta-\alpha}\Gamma(\beta+2)\Gamma(\alpha-\beta-2)}{\Gamma(2)\Gamma(\alpha)[-L]^{\alpha-\beta-2}}. \quad (16)$$

Eventually, we get the OPE side of the three-point correlation function in terms of the selected structures and the perturbative and non-perturbative parts as

$$\Pi_{\mu\alpha\beta}^{OPE} = \Big(\Pi_1^{pert}(q^2) + \Pi_1^{non-pert}(q^2)\Big)q_\alpha g_{\beta\mu} + \Big(\Pi_2^{pert}(q^2) + \Pi_2^{non-pert}(q^2)\Big)q_\mu g_{\beta\alpha} + \Big(\Pi_3^{pert}(q^2) + \Pi_3^{non-pert}(q^2)\Big)P_\mu g_{\beta\alpha} + \Big(\Pi_4^{pert}(q^2) + \Pi_4^{non-pert}(q^2)\Big)\varepsilon_{\lambda\nu\beta\mu}P_\lambda P_\alpha q_\nu + \text{other structures}, \quad (17)$$

where the perturbative parts $\Pi_i^{pert}(q^2)$ can be written in terms of the double dispersion integrals as

$$\Pi_i^{pert}(q^2) = \int ds\int ds'\frac{\rho_i(s,s',q^2)}{(s-p^2)(s'-p'^2)}. \quad (18)$$

The $O(1)$ spectral densities $\rho_i(s,s',q^2)$ are given by the imaginary parts of the $\Pi_i^{pert}(q^2)$ functions, i.e., $\rho_i(s,s',q^2) = \frac{1}{\pi}Im[\Pi_i^{pert}(q^2)]$. After lengthy calculations, the spectral densities corresponding to the selected structures are obtained as

$$\rho_1(s,s',q^2) = \int_0^1 dx\int_0^{1-x} dy\left\{-\frac{3(m_c(4+6y-6x)+m_s(-2+y-x)+2m_b(y-x))}{64\pi^2}\right\}$$

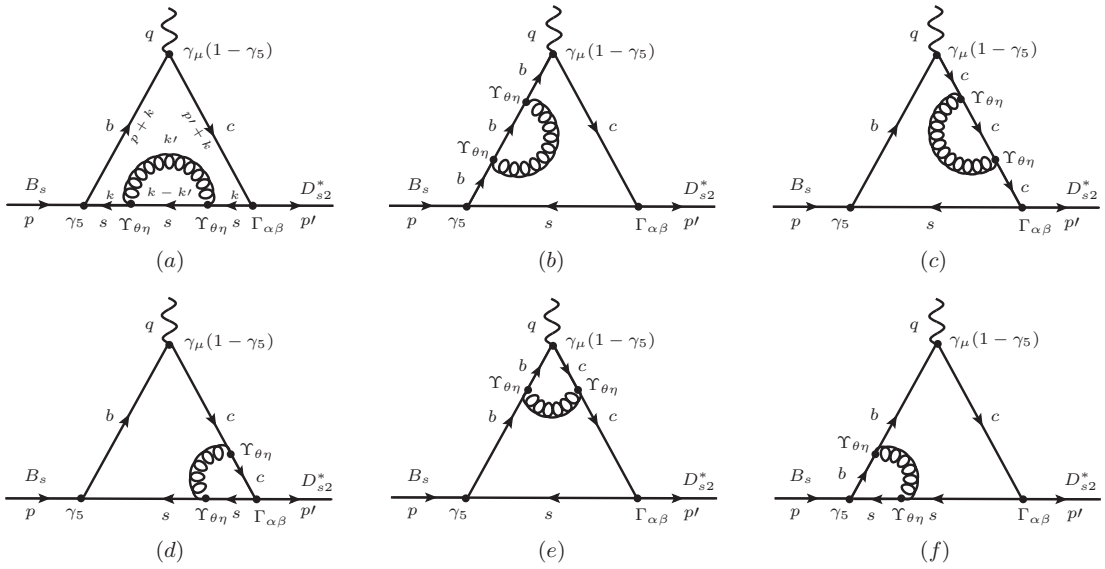

Figure 1: Perturbative $\mathcal{O}(\alpha_s)$ diagrams contributing to the correlation function.

$$
\begin{aligned}
& \times \quad \Theta[L(s,s',q^2)], \\
\rho_2(s,s',q^2) &= \int_0^1 dx \int_0^{1-x} dy \left\{ \frac{3((y-x)(m_b x + m_c(-1+2y+x))}{32\pi^2(-1+y+x)} \right\} \Theta[L(s,s',q^2)], \\
\rho_3(s,s',q^2) &= \int_0^1 dx \int_0^{1-x} dy \left\{ -\frac{3(m_b x(-2+3y+x) + m_c(2y^2+y(-1+x)+(-1+x)x))}{32\pi^2(-1+y+x)} \right\} \\
& \times \quad \Theta[L(s,s',q^2)], \\
\rho_4(s,s',q^2) &= 0,
\end{aligned} \tag{19}
$$

where $\Theta[...]$ is the unit-step function and

$$
L(s,s',q^2) = -m_c^2 y - s'y(x+y-1) - x\Big(m_b^2 - q^2 y + s(x+y-1)\Big). \tag{20}
$$

We also take into account the perturbative $\mathcal{O}(\alpha_s)$ corrections contributing to the correlation function. These corrections for massless quarks are calculated using the standard Cutkosky rules in [25] for calculation of pion form factor with both the pseudoscalar and axial currents. These corrections are also calculated in the case of transition between two infinitely heavy quarks with the spectator quark being massless in [26] using the universal Isgur-Wise function. We calculate the $\mathcal{O}(\alpha_s)$ corrections keeping also the spectator strange quark mass in the calculations. For this aim we consider the diagrams presented in figure 1. As an example we present the amplitude of diagram (a) in figure 1 which is obtained as

$$
\begin{aligned}
\Pi_{\alpha_{s_{(a)}}} &= -16\pi\alpha_s \int \frac{d^4k}{(2\pi)^4} \int \frac{d^4k'}{(2\pi)^4} \\
& \times \quad \frac{Tr\Big[\Gamma_{\alpha\beta}(\not{p}'+\not{k}+m_c)\gamma_\mu(1-\gamma_5)(\not{p}+\not{k}+m_b)\gamma_5(\not{k}+m_s)\gamma^\eta(\not{k}-\not{k}'+m_s)\gamma^\eta(\not{k}+m_s)\Big]}{[(p'^2+k)^2-m_c^2][(p+k)^2-m_b^2][(k-k')^2-m_s^2](k^2-m_s^2)^2 k'^2},
\end{aligned} \tag{21}
$$

where

$$\Gamma_{\alpha\beta}=\gamma_\alpha\left(2k_\beta+p'_\beta\right)+\gamma_\beta\left(2k_\alpha+p'_\alpha\right)-\frac{2}{3}\left(g_{\alpha\beta}-\frac{p'_\alpha p'_\beta}{p'^2}\right)(2\not{k}+\not{p}'). \tag{22}$$

After calculation of the four-integrals appearing in the amplitudes of all diagrams shown in figure 1 and taking the imaginary parts of the obtained results we select the above-mentioned structures to find the $\mathcal{O}(\alpha_s)$ spectral densities $\rho_{\alpha_{s_i}}(s,s',q^2)$. The details of calculations for $\rho_{\alpha_{s_1}}(s,s',q^2)$ are given in appendix A.

The $\Pi_i^{non-pert}(q^2)$ functions are obtained up to five dimension operators. As they have also very lengthy expressions, we do not show their explicit form again.

Having calculated both the hadronic and OPE sides of the correlation function, we match the coefficients of the selected structures from both sides and apply a double-Borel transformation. As a result, we get the following sum rules for the form factors:

$$\begin{aligned}
K(q^2) &= \frac{8(m_b+m_s)}{\Delta}\frac{1}{f_{B_s}f_{D^*_{s2}}m_{D^*_{s2}}m^2_{B_s}}e^{\frac{m^2_{B_s}}{M^2}}e^{\frac{m^2_{D^*_{s2}}}{M'^2}}\\
&\times \left\{\int_{(m_b+m_s)^2}^{s_0}ds\int_{(m_c+m_s)^2}^{s'_0}ds'\left(\rho_1(s,s',q^2)+\rho_{\alpha_{s_1}}(s,s',q^2)\right)e^{-\frac{s}{M^2}}e^{-\frac{s'}{M'^2}}+\hat{B}\Pi_1^{non-pert}\right\},\\
b_-(q^2) &= \frac{12(m_b+m_s)}{f_{B_s}f_{D^*_{s2}}m_{D^*_{s2}}m^2_{B_s}\Delta'}e^{\frac{m^2_{B_s}}{M^2}}e^{\frac{m^2_{D^*_{s2}}}{M'^2}}\\
&\times \left\{\int_{(m_b+m_s)^2}^{s_0}ds\int_{(m_c+m_s)^2}^{s'_0}ds'\left(\rho_2(s,s',q^2)+\rho_{\alpha_{s_2}}(s,s',q^2)\right)e^{-\frac{s}{M^2}}e^{-\frac{s'}{M'^2}}+\hat{B}\Pi_2^{non-pert}\right\}\\
&+ \frac{\Delta}{\Delta'}K(q^2),\\
b_+(q^2) &= \frac{12(m_b+m_s)}{f_{B_s}f_{D^*_{s2}}m_{D^*_{s2}}m^2_{B_s}\Delta'}e^{\frac{m^2_{B_s}}{M^2}}e^{\frac{m^2_{D^*_{s2}}}{M'^2}}\\
&\times \left\{\int_{(m_b+m_s)^2}^{s_0}ds\int_{(m_c+m_s)^2}^{s'_0}ds'\left(\rho_3(s,s',q^2)+\rho_{\alpha_{s_3}}(s,s',q^2)\right)e^{-\frac{s}{M^2}}e^{-\frac{s'}{M'^2}}+\hat{B}\Pi_3^{non-pert}\right\}\\
&- \frac{\Delta-4m^2_{D^*_{s2}}}{\Delta'}K(q^2),\\
h(q^2) &= -i\frac{8(m_b+m_s)}{\Delta-4m^2_{D^*_{s2}}}\frac{1}{f_{B_s}f_{D^*_{s2}}m_{D^*_{s2}}m^2_{B_s}}e^{\frac{m^2_{B_s}}{M^2}}e^{\frac{m^2_{D^*_{s2}}}{M'^2}}\\
&\times \left\{\int_{(m_b+m_s)^2}^{s_0}ds\int_{(m_c+m_s)^2}^{s'_0}ds'\left(\rho_4(s,s',q^2)+\rho_{\alpha_{s_4}}(s,s',q^2)\right)e^{-\frac{s}{M^2}}e^{-\frac{s'}{M'^2}}+B\Pi_4^{non-pert}\right\},
\end{aligned} \tag{23}$$

where M^2 and M'^2 are the Borel mass parameters; and s_0 and s'_0 are continuum thresholds in the initial and final mesonic channels, respectively.

3 Numerical results

In this section we present our numerical results for the transition form factors derived from QCD sum rules and search for the behavior of the these quantities in terms of q^2. To obtain numerical values, we use some input parameters presented in table 1.

Parameters	Values
m_{B_s}	$(5366.77 \pm 0.24)\ MeV$ [27]
$m_{D^*_{s2}(2573)}$	$(2571.9 \pm 0.8)\ MeV$ [27]
f_{B_s}	$(222 \pm 12)\ MeV$ [28]
$f_{D^*_{s2}(2573)}$	(0.023 ± 0.011) [24]
G_F	$1.17 \times 10^{-5}\ GeV^{-2}$
V_{cb}	$(41.2 \pm 1.1) \times 10^{-3}$
$\langle 0\|\overline{s}s\|0\rangle$	$-(0.8 \pm 0.24)^3\ GeV^3$ [29]
$m_0^2(1GeV)$	$(0.8 \pm 0.2)\ GeV^2$ [29]
τ_{B_s}	$(1.465 \pm 0.031) \times 10^{-12} s$ [27]

Table 1: Input parameters used in calculations.

In our calculations, we also use the $\overline{MS}$ quark masses $m_c(m_c) = (1.275 \pm 0.025)\ GeV$, $m_b(m_b) = (4.18 \pm 0.03)\ GeV$ and $m_s(\mu = 2\ GeV) = (95 \pm 5)\ MeV$ [27], and take into account the energy-scale dependence of the $\overline{MS}$ masses from the renormalization group equation to bring the masses to the same scale (see also [30]),

$$\begin{aligned} m_b(\mu) &= m_b(m_b)\left[\frac{\alpha_s(\mu)}{\alpha_s(m_b)}\right]^{\frac{12}{23}}, \\ m_c(\mu) &= m_c(m_c)\left[\frac{\alpha_s(\mu)}{\alpha_s(m_c)}\right]^{\frac{12}{25}}, \\ m_s(\mu) &= m_s(2\ GeV)\left[\frac{\alpha_s(\mu)}{\alpha_s(2\ GeV)}\right]^{\frac{4}{9}}, \end{aligned} \tag{24}$$

where

$$\alpha_s(\mu) = \frac{1}{b_0\ t}\left[1 - \frac{b_1}{b_0^2\ t}\log[t] + \frac{b_1^2\left(\log^2[t] - \log[t] - 1\right) + b_0\ b_2}{b_0^4\ t^2}\right], \tag{25}$$

with

$$\begin{aligned} b_2 &= \frac{1}{128\ \pi^3}\left[2857 - \frac{5033}{9}n_f + \frac{325}{27}n_f^2\right], \\ b_1 &= \frac{1}{24\pi^2}\left(153 - 19n_f\right), \\ b_0 &= \frac{1}{12\pi}\left(33 - 2n_f\right), \\ t &= \log\left[\frac{\mu^2}{\Lambda^2}\right]. \end{aligned} \tag{26}$$

The parameter Λ takes the values $\Lambda = 213\ MeV$, $296\ MeV$ and $339\ MeV$ for the flavors $n_f = 5$, 4 and 3, respectively [27, 30]. We take $n_f = 4$ in the present study. In [30] the authors take $\mu = 1\ GeV$ for the charmed and $\mu = 3\ GeV$ for the bottom tensor mesons. As we have the bottom and charmed mesons respectively in the initial and final states in the transition under consideration, we take the interval $\mu = (2-4)\ GeV$ for this parameter and discuss the rate of changes in the form factors and other observables when going from $\mu = 2\ GeV$ to $\mu = 3\ GeV$ and those from $\mu = 3\ GeV$ to $\mu = 4\ GeV$.

To proceed further, we shall find working regions of the four auxiliary parameters, namely the Borel mass parameters M^2 and M'^2 and continuum thresholds s_0 and s'_0, such that the transition form factors weakly depend on these parameters in those regions. The continuum thresholds s_0 and s'_0 are the energy squares which characterize the beginning of the continuum and depend on the energy of the first excited states in the initial and final channels, respectively. Our numerical calculations point out the following regions for the continuum thresholds s_0 and s'_0: $29\ GeV^2 \leq s_0 \leq 35\ GeV^2$ and $7\ GeV^2 \leq s'_0 \leq 11\ GeV^2$.

The working regions for the Borel mass parameters are calculated demanding that both the higher states and continuum are sufficiently suppressed and the contributions of the operators with higher dimensions are small. As a result, we find the working regions $10\ GeV^2 \leq M^2 \leq 20 GeV^2$ and $5 GeV^2 \leq M'^2 \leq 10 GeV^2$ for Borel mass parameters. To see whether the contributions related to the mesons of interest in the initial and final states have been extracted by considering the above regions for the auxiliary parameters, we calculate the values of functions $-d/d(1/M^2)\ln[\Pi^{OPE}(s_0, s'_0, M^2, M'^2, q^2)]$ and $-d/d(1/M'^2)\ln[\Pi^{OPE}(s_0, s'_0, M^2, M'^2, q^2)]$ in the Borel scheme. Taking into account all the input parameters we find the values $29.44\ GeV^2 \sim m^2_{B_s}$ and $5.58\ GeV^2 \sim m^2_{D^*_{s2}(2573)}$ for these functions, respectively, showing that the contributions of the related mesons in the initial and final states have been roughly extracted. We show, as an example, the dependence of the form factor $K(q^2)$ at $q^2 = 1$ on the Borel mass parameters M^2 and M'^2 in figure 2. With a quick look at this figure, we see that not only this form factor depicts weak dependence on the Borel parameters on their working regions, but the perturbative contribution constitutes the main part of the total value.

	f_0	σ_1	σ_2
$K(q^2)$	0.70 ± 0.30	-0.93 ± 0.26	-1.93 ± 0.58
$b_-(q^2)$	$(0.072 \pm 0.031)\ GeV^{-2}$	3.22 ± 0.97	-1.72 ± 0.82
$b_+(q^2)$	$(-0.031 \pm 0.013)\ GeV^{-2}$	4.07 ± 1.22	1.39 ± 0.41
$h(q^2)$	$(-0.0092 \pm 0.0038)\ GeV^{-2}$	0.33 ± 0.10	-0.43 ± 0.12

Table 2: Parameters appearing in the fit function of the form factors at $\mu = 2\ GeV$.

At this stage, we would like to find the behaviors of the considered form factors in terms of q^2 using the working regions for the continuum thresholds and Borel mass parameters. Our calculations depict that the form factors are truncated at $q^2 \simeq 7\ GeV^2$. To extend the results to the whole physical region, we have to find a fit function such that it coincide with

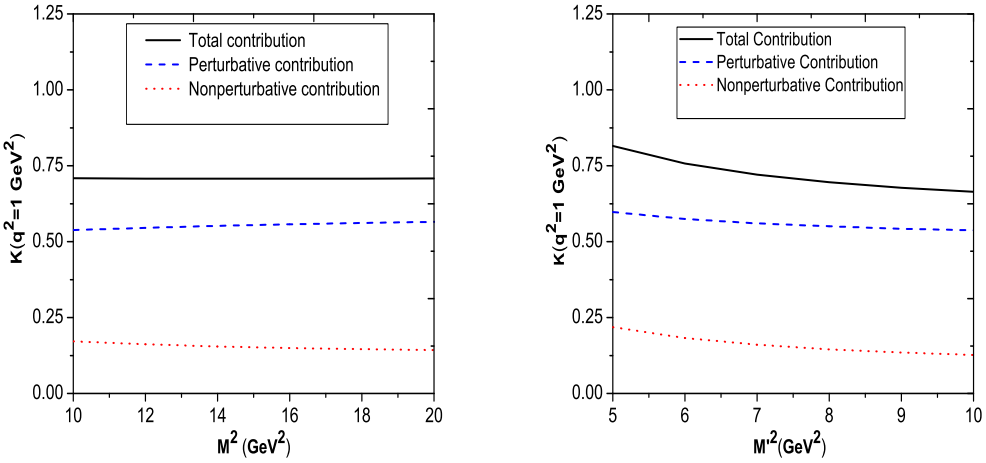

Figure 2: **Left:** K($q^2 = 1$) as a function of the Borel mass M^2 at average values of the s_0, s_0' and M'^2. **Right:** K($q^2 = 1$) as a function of the Borel mass M'^2 at average values of the s_0, s_0' and M^2.

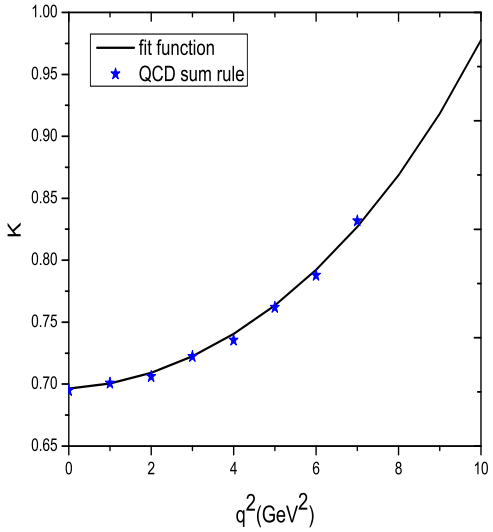

Figure 3: $\mathbf{K}(q^2)$ as a function of q^2 at $M^2 = 15GeV^2$, $M'^2 = 7.5GeV^2$, $s_0 = 35GeV^2$ and $s_0' = 9GeV^2$.

the QCD sum rules results at $q^2 = (0-7)\ GeV^2$ region. Here, we should also stress that at the time-like momentum transfers the spectral representations mainly develop anomalous contributions, i.e., the double spectral densities receive contributions beyond those due to Landau-type singularities and deviate from the corresponding Feynman amplitudes. This problem is discussed in details in [31]. Although these contributions do not affect the values

of the form factors at $q^2=0$ and turn out to be small at higher values of q^2 by the above-mentioned ranges of the auxiliary parameters in the decay channel under consideration, we take also into account these small contributions in our numerical calculations. We find that the form factors are well fitted to the following function (see figure 3)[32]:

$$f(q^2)=\frac{f_0}{\Big(1-\frac{q^2}{m^2_{B_s}}\Big)\Big[1-\sigma_1\Big(\frac{q^2}{m^2_{B_s}}\Big)+\sigma_2\Big(\frac{q^2}{m^2_{B_s}}\Big)^2\Big]}, \tag{27}$$

where the values of the parameters f_0, σ_1 and σ_2, as an example at $\mu=2\,GeV$, are presented in table 2. The quoted errors in the results are due to the errors in determinations of the working regions of the continuum thresholds, Borel mass parameters as well as uncertainties coming from other input parameters. Our numerical analysis show that setting μ from $2\ GeV$ to $3\ GeV$ increases the values of the form factors roughly with amount of 35% at a fixed value of q^2. This rate of increase in the values of the form factors are roughly 25% when going from $\mu=3\ GeV$ to $\mu=4\ GeV$. These rates of changes reveal that the form factors depend on the scale parameter μ, considerably.

In this part we would like to discuss the constraints that the HQET limit provides on the form factors under discussion as the considered decay channel is based on the heavy-to-heavy $b\to c$ transition at quark level. Taking into account all the definitions and the values of the related parameters discussed in [33] (and references therein) for a similar channel, namely $B_s\to D_{sJ}(2460)l\nu$, we find that the HQET limit affects the form factors $h(0)$ and $K(0)$ more than the form factors $b_+(0)$ and $b_-(0)$ such that the values of the form factors $h(0)$ and $K(0)$ decrease by 35% and 42%, respectively. In contrast, the form factors $b_+(0)$ and $b_-(0)$ increase by 16% and 5%, respectively.

Having found the fit function of the form factors in terms of q^2 at full physical region, now we calculate the decay width of the process under consideration. The differential decay width for $B_s\to D^*_{s2}(2573)\ell\bar{\nu}_\ell$ transition is obtained as (see also [34])

$$\begin{aligned}
\frac{d\Gamma}{dq^2} &= \frac{\lambda(m^2_{B_s},m^2_{D^*_{s2}},q^2)}{4m^2_{D^*_{s2}}}\Big(\frac{q^2-m^2_\ell}{q^2}\Big)^2\frac{\sqrt{\lambda(m^2_{B_s},m^2_{D^*_{s2}},q^2)}G_F^2V_{cb}^2}{384m^3_{B_s}\pi^3}\Big\{\frac{1}{2q^2}\Big[3m^2_\ell\lambda(m^2_{B_s},m^2_{D^*_{s2}},q^2)[V_0(q^2)]^2\\
&+ (m^2_\ell+2q^2)\Big|\frac{1}{2m_{D^*_{s2}}}\Big[(m^2_{B_s}-m^2_{D^*_{s2}}-q^2)(m_{B_s}-m_{D^*_{s2}})V_1(q^2)-\frac{\lambda(m^2_{B_s},m^2_{D^*_{s2}},q^2)}{m_{B_s}-m_{D^*_{s2}}}V_2(q^2)\Big]\Big|^2\Big]\\
&+ \frac{2}{3}(m^2_\ell+2q^2)\lambda(m^2_{B_s},m^2_{D^*_{s2}},q^2)\Big[\Big|\frac{A(q^2)}{m_{B_s}-m_{D^*_{s2}}}-\frac{(m_{B_s}-m_{D^*_{s2}})V_1(q^2)}{\sqrt{\lambda(m^2_{B_s},m^2_{D^*_{s2}},q^2)}}\Big|^2\\
&+ \Big|\frac{A(q^2)}{m_{B_s}-m_{D^*_{s2}}}+\frac{(m_{B_s}-m_{D^*_{s2}})V_1(q^2)}{\sqrt{\lambda(m^2_{B_s},m^2_{D^*_{s2}},q^2)}}\Big|^2\Big]\Big\},
\end{aligned} \tag{28}$$

where

$$\begin{aligned}
A(q^2) &= -(m_{B_s}-m_{D^*_{s2}})h(q^2),\\
V_1(q^2) &= -\frac{K(q^2)}{m_{B_s}-m_{D^*_{s2}}},
\end{aligned}$$

$$
\begin{aligned}
V_2(q^2) &= (m_{B_s} - m_{D^*_{s2}})b_+(q^2), \\
V_0(q^2) &= \frac{m_{B_s} - m_{D^*_{s2}}}{2m_{D^*_{s2}}}V_1(q^2) - \frac{m_{B_s} + m_{D^*_{s2}}}{2m_{D^*_{s2}}}V_2(q^2) - \frac{q^2}{2m_{D^*_{s2}}}b_-(q^2), \\
\lambda(a,b,c) &= a^2 + b^2 + c^2 - 2ab - 2ac - 2bc.
\end{aligned} \tag{29}
$$

Performing the integral over q^2 in the above equation at whole physical region, finally, we obtain the values of the total decay widths and branching ratios for all lepton channels as presented in tables 3, 4 and 5 for $\mu = 2\ GeV$, $\mu = 3\ GeV$ and $\mu = 4\ GeV$, respectively. From these tables we see that when setting μ from 2 GeV to 3 GeV, the decay rate and branching ratio increase by roughly 82%, but when going from $\mu = 3\ GeV$ to $\mu = 4\ GeV$ the rate of increase in these quantities is roughly 40% for all lepton channels. From these changes, we conclude that the results of these quantities also depend considerably on the scale parameter μ. The orders of branching fractions show that the semileptonic $B_s \to D^*_{s2}(2573)\ell\overline{\nu}_\ell$ is accessible, experimentally at all lepton channels in near future.

	$\Gamma(GeV)$	Br
$B_s \to D^*_{s2}(2573)\tau\overline{\nu}_\tau$	$(2.82 \pm 1.32) \times 10^{-16}$	$(5.08 \pm 2.38) \times 10^{-4}$
$B_s \to D^*_{s2}(2573)\mu\overline{\nu}_\mu$	$(5.37 \pm 2.44) \times 10^{-16}$	$(1.19 \pm 0.54) \times 10^{-3}$
$B_s \to D^*_{s2}(2573)e\overline{\nu}_e$	$(5.41 \pm 2.48) \times 10^{-16}$	$(1.21 \pm 0.55) \times 10^{-3}$

Table 3: Numerical results for the decay widths and branching ratios at different lepton channels for $\mu = 2\ GeV$.

	$\Gamma(GeV)$	Br
$B_s \to D^*_{s2}(2573)\tau\overline{\nu}_\tau$	$(5.14 \pm 2.46) \times 10^{-16}$	$(9.26 \pm 4.33) \times 10^{-4}$
$B_s \to D^*_{s2}(2573)\mu\overline{\nu}_\mu$	$(9.79 \pm 4.45) \times 10^{-16}$	$(2.18 \pm 0.98) \times 10^{-3}$
$B_s \to D^*_{s2}(2573)e\overline{\nu}_e$	$(9.86 \pm 4.52) \times 10^{-16}$	$(2.20 \pm 0.92) \times 10^{-3}$

Table 4: Numerical results for the decay widths and branching ratios at different lepton channels for $\mu = 3\ GeV$.

In summary, taking into account the perturbative $\mathcal{O}(\alpha_s)$ corrections we have calculated the transition form factors governing the semileptonic $B_s \to D^*_{s2}(2573)\ell\bar{\nu}_\ell$ transition at all lepton channels using an appreciate three-point correlation function. The fit functions of the form factors have been used to estimate the corresponding decay widths and branching ratios. The orders of branching ratios indicate that such channels contribute to the total width of the B_s meson, considerably. We hope that it will be possible to study these channels at LHCb in near future. Comparison of the future data with the theoretical results can help us in understanding the internal structure and nature of the $D^*_{s2}(2573)$ charmed-strange tensor meson.

	$\Gamma(GeV)$	Br
$B_s \to D^*_{s2}(2573)\tau\overline{\nu}_\tau$	$(7.20 \pm 3.38) \times 10^{-16}$	$(1.30 \pm 0.61) \times 10^{-3}$
$B_s \to D^*_{s2}(2573)\mu\overline{\nu}_\mu$	$(1.37 \pm 0.62) \times 10^{-15}$	$(3.06 \pm 1.39) \times 10^{-3}$
$B_s \to D^*_{s2}(2573)e\overline{\nu}_e$	$(1.39 \pm 0.64) \times 10^{-15}$	$(3.08 \pm 1.40) \times 10^{-3}$

Table 5: Numerical results for the decay widths and branching ratios at different lepton channels for $\mu = 4\ GeV$.

3.1 ACKNOWLEDGEMENT

This work has been supported by the Scientific and Technological Research Council of Turkey (TUBITAK) under the research project 114F018.

References

[1] P. del Amo Sanchez et al. [BABAR Collaboration], "Study of $B \to \pi l\nu$ and $B \to \rho l\nu$ Decays and Determination of $|Vub|$ ", Phys. Rev. D 83, 032007 (2011), arXiv:1005.3288 [hep-ex].

[2] T. Hokuue et al. [Belle Collaboration],"Measurements of branching fractions and q^2 distributions for $B \to \pi l\nu$ and$B \to \rho l\nu$ Decays with $B \to D^*(2536)l\nu$ Decay Tagging", Phys. Lett. B 648:139 (2007), [arXiv:hep-ex/0604024].

[3] P. del Amo Sanchez et al. [BABAR Collaboration], "Search for the Rare Decay $B \to \nu\bar{\nu}$ ", Phys. Rev. D 82, 112002 (2010), arXiv:1009.1529 [hep-ex].

[4] R. Aaij et al. [LHCb Collaboration], "First observation of the decay $B^+ \to \pi^+\mu^+\mu^-$". J. High Energy Phys. 12, 125 (2012), arXiv:1210.2645 [hep-ex].

[5] J. P. Lees et al. [BABAR Collaboration], "Evidence for an Excess of $\bar{B} \to D^*\tau^-\bar{\nu}_\tau$ Decays" Phys. Rev. Lett. 109, 101802 (2012), arXiv:1205.5442 [hep-ex].

[6] A. Bozek (for Belle Collaboration), "The $B \to \tau\nu$ and $B \to \bar{D}^*\tau^+\bar{\nu}_\tau$ measurements", talk given at FPCP 2013, May 3-6, 2013, Buzios, Breizl (2013).

[7] S. Fajfer, Kamenik J F, Nisandzic I, "On the $B \to D^*\tau\bar{\nu}_\tau$ Sensitivity to New Physics", Phys. Rev. D 85(09), 094025 (2012), arXiv:1203.2654 [hep-ph].

[8] P. Biancofiore, P. Colangelo, F. De Fazio, "On the anomalous enhancement observed in $B \to D^{(}*)\tau\bar{\nu}_\tau$ decays", Phys. Rev. D 87, 074010 (2013), arXiv:1302.1042 [hep-ph].

[9] D. Becirevic, N. Kosnik, A. Tayduganov, "$B \to D\tau\bar{\nu}_\tau$ vs. "$B \to D\mu\bar{\nu}_\mu$", Phys. Lett. B 716, 208 (2012), arXiv:1206.4977 [hep-ph].

[10] E. Gamiz et al., "Neutral B Meson Mixing in Unquenched Lattice QCD", Phys. Rev. D 80, 014503 (2009), arXiv:0902.1815[hep-ph].

[11] K.-C. Yang, "B to Light Tensor Meson Form Factors Derived from Light-Cone Sum Rules" Phys. Lett. B 695, 444 (2011), arXiv:1010.2944[hep-ph].

[12] J. P. Lees et al. [BaBar Collaboration], "Measurement of the semileptonic branching fraction of the B_s meson", Phys. Rev. D 85, 011101 (2012), arXiv:1110.5600 [hep-ex]

[13] A. Aaij et al. [LHCb collaboration], "First evidence for the decay $B_s^0 \to \mu^+\mu^-$", Phys. Rev. Lett. 110, 021801, (2013), arXiv:1211.2674 [hep-ex].

[14] R. Aaij et al. [LHCb Collaboration], "First measurement of the CP-violating phase in $B_s^0 \to \varphi\varphi$ decays", Phys. Rev. Lett. 110, 241802 (2013), arXiv:1303.7125 [hep-ex].

[15] V. M. Abazov et al. [D0 Collaboration], "Measurement of the Semileptonic Branching Ratio of B_s^0 to an Orbitally Excited $D_s^{*}*$ State: $Br(B_s^0 \to D_{s1}^-(2536)\mu^+\nu_\mu X)$" Phys. Rev. Lett. 102, 051801 (2009), arXiv:0712.3789 [hep-ex].

[16] E. B. Gregory et al., "Precise B , B_s and B_c meson spectroscopy from full lattice QCD", Phys. Rev. D 83, 014506 (2011), arXiv:1010.3848[hep-ph].

[17] L.-F. Gan, M.-Q. Huang, "QCD Sum Rule Analysis of Semileptonic B_{s1}, B_{s2}^*, B_{s0}^*, and B_{s1}' Decays in HQET", arXiv:1009.0980[hep-ph].

[18] C. Albertus, E. Hernandez, J. Nieves, C. Hidalgo-Duque, "B_s mesons: semileptonic and nonleptonic decays", Contribution to the proceedings of the MESON 2014 Conference, arXiv:1410.0820 [hep-ph].

[19] M. Steinhauser, "$B_s \to \mu^+\mu^-$ and $\bar{B} \to X_s\gamma$ to NNLO ", contribution to the proceedings of Loops and Legs in Quantum Field Theory, 27 April - 2 May 2014, Weimar, Germany, arXiv:1406.6787 [hep-ph].

[20] C. M. Bouchard, G. P. Lepage, C. Monahan, H. Na, J. Shigemitsu, "$B_s \to K\ell\nu$ form factors from lattice QCD", Phys. Rev. D 90, 054506 (2014).

[21] C. Albertus, "Semileptonic and nonleptonic decays of B_s mesons ", Contribution to the proceedings of the 22nd European Conference on Few Body Problems in Physics (EFB22), arXiv:1403.2719 [hep-ph].

[22] M. A. Shifman, A. I. Vainshtein and V. I. Zakharov, "QCD and Resonance Physics", Nucl. Phys. B 147, 385 (1979).

[23] K. Azizi, H. Sundu, S. Sahin, "Investigation of the semileptonic transition of the B into the orbitally excited charmed tensor meson", Phys. Rev. D 88, 03600 (2013), arXiv:1306.4098 [hep-ph].

[24] K. Azizi, H. Sundu, J. Y. Sungu, N. Yinelek, "Properties of $D_{s2}^*(2573)$ charmed-strange tensor meson", Phys. Rev. D 88, 036005 (2013); Phys. Rev. D 88, 099901(E), (2013), arXiv:1307.6058[hep-ph].

[25] V.V.Braguta and A.I.Onishchenko, "Pion form factor and QCD sum rules: case of pseudoscalar current", Phys. Lett. B 591, 255 (2004), arXiv:hep-ph/0311146; "Pion form factor and QCD sum rules: case of axial current", Phys. Lett. B 591, 267 (2004), arXiv:hep-ph/0403240.

[26] P. Colangelo, F. De Fazio, N. Paver, "Universal $\tau_{1/2}(y)$ Isgur-Wise function at the next-to-leading order in QCD sum rules ", Phys. Rev. D 58, 116005 (1998), arXiv:hep-ph/9804377.

[27] K. A. Olive et al. (Particle Data Group), "The Review of Particle Physics", Chin. Phys. C, 38, 090001 (2014).

[28] M. J. Baker, J. Bordes, C. A. Dominguez, J. Penarrocha, K. Schilcher, "B Meson Decay Constants f_{B_c}, f_{B_s} and f_B from QCD Sum Rules", JHEP 1407, 032 (2014).

[29] L. J. Reinders, H. Rubinstein and S. Yazaki,"Hadron Properties From QCD Sum Rules", Phys. Rept. 127, 1 (1985).

[30] Z.-G. Wang, "Strong Decay of the heavy tensor mesons with QCD sum rules", Eur. Phys. J. C 74, 3123 (2014).

[31] P. Ball, V. M. Braun, H. G. Dosch, "Form factors of semileptonic D decays from QCD sum rules ", Phys. Rev. D 44, 3567 (1991).

[32] D. Melikhov and B. Stech, "Weak form factors for heavy meson decays: an update", Phys.Rev. D 62, 014006 (2000).

[33] T. M. Aliev, K. Azizi, A. Ozpineci, "Semileptonic $B_s \to D_{sJ}(2460) l\nu$ decay in QCD", Eur. Phys. J. C 51, 593 (2007).

[34] X.-X. Wang, W. Wang and C.-D. Lu, "B_c to p-wave charmonia transitions in the covariant light-front approach" Phys. Rev. D 79, 114018 (2009).

Appendix

In this appendix, as an example, we briefly show how we calculate the perturbative $\mathcal{O}(\alpha_s)$ corrections for the structure $q_\alpha g_{\beta\mu}$, i.e., $\rho_{\alpha_{s_1}}(s,s',q^2)$. After performing the trace of Eq. (21) and taking into account also the contributions of all diagrams in figure 1, we use the Feynman parametrization to perform the four-k and four-k' integrals. First we perform the four integral over k. Using the Feynman parametrization, as an example for diagram (a) in figure 1, one can write

$$\begin{aligned}\frac{1}{A_1^a A_2^b A_3^c A_4^d A_5^e} &= \frac{\Gamma[a+b+c+d+e]}{\Gamma[a]\Gamma[b]\Gamma[c]\Gamma[d]\Gamma[e]}\int_0^1 dx\int_0^1 dy\int_0^1 dz\int_0^1 dt\int_0^1 dt' \\ &\times \frac{x^{a-1}y^{b-1}z^{c-1}t^{d-1}t'^{e-1}}{\{xA_1+yA_2+zA_3+tA_4+t'A_5\}^{a+b+c+d+e}}\delta(x+y+z+t+t'-1),\end{aligned} \tag{30}$$

where $A_1=[(p'+k)^2-m_c^2]$, $A_2=[(p+k)^2-m_b^2]$, $A_3=[(k-k')^2-m_s^2]$, $A_4=[k^2-m_s^2]$, $A_5=k'^2$ and $a=b=c=d=e=1$ for diagram (a). The next step is to perform the integral over t' using the DiracDelta in Eq. (30), rearrange the denaminator of the integrand on the right-hand side of this equation and use the shift

$$k\to k-\frac{py+p'x-k'z}{x+y+z+t}, \tag{31}$$

to make the denaminator full-squared in terms of k, i.e., in the form of $k^2-\Delta$, where Δ is a function of k', p, p', x, y, z, t and quark masses.

The integral over k is performed via the following table of $D-$dimensional integrals:

$$\begin{aligned}\int\frac{d^Dk}{(2\pi)^D}\frac{1}{(k^2-\Delta)^n} &= \frac{i(-1)^n}{(4\pi)^{D/2}}\frac{\Gamma[n-D/2]}{\Gamma[n]}\Big(\frac{1}{\Delta}\Big)^{n-D/2}, \\ \int\frac{d^Dk}{(2\pi)^D}\frac{k^2}{(k^2-\Delta)^n} &= \frac{i(-1)^{n-1}}{(4\pi)^{D/2}}\frac{D}{2}\frac{\Gamma[n-D/2-1]}{\Gamma[n]}\Big(\frac{1}{\Delta}\Big)^{n-D/2-1}, \\ \int\frac{d^Dk}{(2\pi)^D}\frac{k^\mu k^\nu}{(k^2-\Delta)^n} &= \frac{i(-1)^{n-1}}{(4\pi)^{D/2}}\frac{g^{\mu\nu}}{2}\frac{\Gamma[n-D/2-1]}{\Gamma[n]}\Big(\frac{1}{\Delta}\Big)^{n-D/2-1}, \\ \int\frac{d^Dk}{(2\pi)^D}\frac{(k^2)^2}{(k^2-\Delta)^n} &= \frac{i(-1)^n}{(4\pi)^{D/2}}\frac{D(D+2)}{4}\frac{\Gamma[n-D/2-2]}{\Gamma[n]}\Big(\frac{1}{\Delta}\Big)^{n-D/2-2}, \\ \int\frac{d^Dk}{(2\pi)^D}\frac{k^\mu k^\nu k^\rho k^\sigma}{(k^2-\Delta)^n} &= \frac{i(-1)^n}{(4\pi)^{D/2}}\frac{\Gamma[n-D/2-2]}{\Gamma[n]}\Big(\frac{1}{\Delta}\Big)^{n-D/2-2} \\ &\times \frac{1}{4}(g^{\mu\nu}g^{\rho\sigma}+g^{\mu\rho}g^{\nu\sigma}+g^{\mu\sigma}g^{\nu\rho}).\end{aligned} \tag{32}$$

Now, we proceed to perform the four-integral over k'. Again we try to make the denaminator of the integrand of the integration over k' full-squared in terms of k' viz. $k'^2-\Delta'$, with Δ' being a function of p, p', x, y, z, t and quark masses, by using the shift:

$$k'\to k'-\frac{(py+p'x)z}{x+y+z-t^2-z^2-(x+y)(x+y+z)-t(2x+2y+z-1)}. \tag{33}$$

In this step, the integral over k' is performed again using the above table of $D-$dimensional integrals. Now, we come back to the four dimensions. For the terms which converge we directly set $D = 4$, but for those that diverge by setting $D = 4$, the following relation is used:

$$\frac{\Gamma[2 - D/2]}{(4\pi)^{D/2}}\Big(\frac{1}{\Delta'}\Big)^{2-D/2} = \frac{1}{(4\pi)^2}\Big(\frac{2}{\epsilon} - \log\Delta' - \gamma + \log(4\pi) + \mathcal{O}(\epsilon)\Big), \tag{34}$$

with $\epsilon = 4 - D$ and Δ' is negative. To obtain the imaginary part, we use the following relation:

$$\log\Big[-|\Delta'|\Big] = \log\Big[e^{i\pi}|\Delta'|\Big] = i\pi + \log\Big[|\Delta'|\Big]. \tag{35}$$

We do the similar calculations for all diagrams in figure 1. As a result, we obtain

$$\begin{aligned}
\rho_{\alpha_{s_1}} &= \alpha_s\int_0^1 dx\int_0^{1-x} dy\int_0^{1-x-y} dz\int_0^{1-x-y-z} dt\Big\{\frac{1}{4\pi^3\Lambda^5}\Big[-t(x+y+t-1)\Big((x+y+t-1)^2\\
&\times (6m_c(t-3x+5y)+m_b(3t-5x+11y))+z(x+y+t-1)\Big(m_b(6t-2x+14y-3)\\
&+ 2m_s(5x-11y-3t)-6m_c(2x-6y-2t+1)\Big)+6z^2(x+y+t-1)(m_b-m_s+2m_c)\\
&+ 3z^3(m_b+2m_c-2m_s)\Big)\Theta\Big[L_1[s,s',q^2,x,y,z,t]\Big]\\
&+ y(x+y+t-1)\Big((x+y+t-1)^2(24m_c(x-y)+m_s(t-7x+9y))+z(x+y+t-1)\\
&\times (24m_c(1-t-2y)-2m_b(t-7x+9y)+m_s(2x+18y+10t-2))-6z^2(x+y+t-1)\\
&\times (3m_b+8m_c-3m_s)-3z^3(6m_b+8m_c-3m_s)\Big)\Theta\Big[L_2[s,s',q^2,x,y,z,t]\Big]\\
&+ x(x+y+t-1)\Big((x+y+t-1)^2(m_s-m_b)(5t-3x+13y)-z(x+y+t-1)\\
&\times \Big(24m_c(t-x+3y)+(3+2t-6x+10y)(m_b-m_s)\Big)+6z^2(x+y+t-1)\\
&\times (m_b+4m_c-m_s)+3z^3(m_b+8m_c-m_s)\Big)\Theta\Big[L_3[s,s',q^2,x,y,z,t]\Big]\Big]\\
&+ \int_0^{1-x-y-z-t} dw\Big[\frac{1}{4\pi^3\Lambda^5}\Big(m_b(t^2+wr-3x+3x^2+w(3x+y-1)+y+2xy-y^2+z\\
&+ 3xz-yz-z^2+t(4x+z+w-1))(12+11t^2+11w^2-23x-23y+23w(x+y-1)\\
&+ 11(x+y)^2-23z+22wz+23z(x+y)+11z^2+t(22x+22y+23z+23w-23))+m_c\\
&\times (4t^4+w^4+2(x+y-1)^2(11x^2+y(9-7y)+x(4y-15))+z(x+y-1)(51x^2+y\\
&\times (57-37y)+x(14y-43)-18)+z^2(43+12x-44y)(x+y-1)-2z^3(13x+15y-16)\\
&- 7z^4+t^3(11w+34x-2y+7z-14)+w^2(13+40x^2-16y^2+3y-28yz+x(24y-6z\\
&- 53)+2z(8-9z))+w(73x-122x^2+55x^3-27y-56xy+77x^2y+66y^2-11xy^2-33y^3\\
&+ 2z(x+y-1)(15+26x-30y)-2z^2(21x+27y-28)-20z^3-6)+2w^3(5x+3y+2z\\
&- 4)+t^2(16+12w^2+78x^2+6y(3-5y)-23yz-16z^2+x(48y+65z-102)+w(77x\\
&- 11y-4(7+z)))+t(8w^3+2(x+y-1)(3+35x^2+y(20-19y)+2x(8y-23))+w^2
\end{aligned}$$

$$
\begin{aligned}
&\times\ (52x-4y-12z-25)+z(109x^2+y(97-67y)+x(42y-94))+z^2(59-4x-60y)\\
&-\ 28z^3+w(23+121x^2+38y-55y^2+34z-64yz-48z^2+6x(11y+8z-25))))-m_s\\
&\times\ (2t^4+11w^4+(x+y-1)^2(8x^2+y(5-4y)+x(4y-11))+z(x+y-1)(56x^2-55x\\
&+\ 21y+40xy-16y^2-5)+z^2(x+y-1)(17+81x-23y)+z^3(19+25x-19y)-7z^4\\
&+\ t^3(14x+2y+20z+16w-7)+w^3(47x+3y+26z-25)+w(60x-3-109x^2+52x^3\\
&-\ 16y-70xy+84x^2y+39y^2+12xy^2-20y^3+16z(x+y-1)(10x-3y)+z^2(13+97x\\
&-\ 35y)-10z^3)+t^2(8+27w^2+30xr-y(1+6y)-37z+24yz+29z^2+w(84x+12y\\
&+\ 56z-35)+x(24y+96z-41))+w^2(17+79x^2+8y-31z-(y+z)(25y-12z)+x\\
&\times\ (54y+119z-96))+t(25w^3+26x^3-6y+y^2(19-10y)-3)+12z-12y^2z+6z^2\\
&\times\ (y-2)+3z^3+w^2(106x+2y+53z-44)+x^2(42y+132z-61)+2x(19+3y(y-7)\\
&-\ 7z+60yz+55z^2)+w(22+120x^2-24y^2+y(4+8z)+24x(4y+9z-6)+31z^2\\
&-\ 56z))\Big)\Theta\Big[L_4[s,s',q^2,x,y,z,t,w]\Big]+\frac{1}{4\pi^3\Lambda''^5}\Big(m_b(-6t^4+(x+y-1)^2(33x^2+y(7-11y)\\
&+\ x(22y-9))+z(x+y-1)(9+75x^2-y(13+29y)+x(46y-57))+z^2(24+81x^2+15x\\
&\times\ (6y-7)+y(9y-65))+3z^3(16x+12y-7)+6z^4+w^3(18x+6y+6z-1)-t^3(12x\\
&+\ 24y+12z+18w-19)+t^2(37x^2-18w^2+y(55-35y-12z)+17z-w(6x+42y+18z\\
&-\ 37)+x(15+2y+24z)-20)+w^2(2+59x^2-13y^2+z(18z-23)+y(48z-5)+x(46y\\
&+\ 84z-45))+t(7-6w^3+75x^3+w^2(17+24x-12y)+y(60y-29y^2-38))+4z-2yz\\
&\times\ (5+13y)+z^2(48y-23)+12z^3+x^2(121y+118z-88)+x(6-28y+17y^2-90z\\
&+\ 92yz+84z^2)+2w(48x^2+25y-24y^2-3z+18yz+9z^2+3x(8y+18z-5))+w(75x^3\\
&-\ 29y^3+y^2(38-4z)+2y(z-1)(4+39z)+x^2(121y+140z-110)+(z-1)(1-25z\\
&+\ 18z^2)+x(17y^2+8y(17z-9)+6(z-1)(19z-6))))+m_s(17t^4-5w^4-(x+y-1)^2\\
&\times\ (27x^2+10x(y-3)+18y-17y^2)+w^3(16-38x+6y-42z)-2z(x+y-1)(15+42x^2\\
&+\ 13y(1-2y)+x(16y-57))-z^2(x+y-1)(111x-25y-87)-4z^3(21x+10y-21)\\
&-\ 27z^4+t^3(8x+52y+24z+46w-52)+t^2(53+36w^3-67x^2-22w(4+x-5y)+69y^2\\
&-\ 122y+2x(7+y-34z)-20z+6wz+64yz-30z^2)+2w(3-49x+88x^2-42x^3+21y\\
&+\ 38xy-58x^2y-50y^2+10xy^2+26y^3-4z(x+y-1)(25x-9y-13)+y(30+28z)+2x\\
&\times\ (21y+80z-53))+2t(w^3-42x^3+(y-1)^2(26y-9)+x^2(77-58y-89z)+z(y-1)\\
&\times\ (17+47y)+2z^2(29-7y)-32z^3-2w^2(5+17x-16y+15z)+2x(8y+5y^2+53z\\
&-\ 21yz-40z^2-13)+w(18-78x^2-76y+58y^2+48z+18yz-63z^2-2x(10y+57z\\
&-\ 30))))+m_c\{10w^4-8t^4+(x+y-1)^2(x^2-3y(y-4)-2x(y+18))+z(x+y-1)\\
&\times\ (36+38x^2+31y-18y^2-101x+20xy)+2z^2(50+33x^2-y(23+11y)+x(22y-83))\\
&+\ z^3(65x+29y-92)+28z^4+t^3(28-14w+13x-23y+4z)+w^3(39x+3y+58z-32)\\
&+\ t^2(62x^2-26y^2+6w^2+58y-36z-17yz+60z^2+w(24+65x-43y+66z)+x(36y\\
&+\ 91z-62)-32)+w^2(34+64x^2+6y-24y^2-156z+35yz+114z^2+x(40y+143z\\
&-\ 114))+w(38x^3-18y^3+y^2(51-46z)+y(z-1)(21+61z)+x^2(58y+130z-137)\\
&+\ x(111+2y(y-43)-280z+84yz+169z^2)+2(z-1)(6-61z+47z^2))+t[12+22w^3
\end{aligned}
$$

$$
\begin{aligned}
&+ \quad 38x^3 - 47y + y^2(53 - 18y) + 68z + 12yz(1 - 4y) + z^2(35y - 156) + 76z^3 + w^2(91x - 17y \\
&+ \quad 120z - 36) + x^2(58y + 128z - 135) + x(85 + 2y(y - 41) - 228z + 80yz + 143z^2) + 2w \\
&\times \quad (1 + 63x^2 + 32y - 25y^2 - 96z + 9yz + 87z^2 + x(38y + 117z - 88))]\}\Big) \\
&\times \quad \Theta\Big[L_5[s, s', q^2, x, y, z, t, w]\Big] \\
&- \quad \frac{1}{4\pi^3\Lambda'''^5}\Big(m_b(-11t^4 - 3(x^2 + x(y - 1) + y(y - 1))(3 + x(16 + 11x) - 5y - 16xy + 2y^2) \\
&+ \quad z(15x^3 + 2x(y - 1)(22 + 29y) + x^3(62y - 92) + y^2(23 - 12y) - 4y - 7) + z^2(20 + xz^2(61 \\
&+ \quad 53x - 10y) - 17y) + z^3(12y - 26x - 19) + 6z^4 + 3t^3(w + y + z - 22x - 1) + w^3(1 + 8x \\
&- \quad 6y + 6z) + t^2(3w^2 - 132x^2 + w(21x - 16y + 28z - 16) + 21x(y + z - 1) - (13 + 19y \\
&- \quad 25z)(y + z - 1)) + w^2(31x^2 + y(23 - 18y) + x(58y - 10z - 7) + z(18z - 17)) + w(15x^3 \\
&+ \quad 2x(5 + 46y - 22z)(y + z - 1) + x^2(40y + 84z - 70) - (y + z - 1)(1 + y(18y - 25) + z(19 \\
&- \quad 18z))) + t(14w^3 - 110x^3 + 33x^2(y + z - 1) - 2x(y + z - 1)(26 + 5y - 39z) + (y + z - 1)^2 \\
&\times \quad (1 + 48y - 20z) + w^2(34x + 76y + 8z - 27) + w(33x^2 + 2(y + z - 1)(55y - 13z - 6) + 2x \\
&\times \quad (12y + 56z - 43)))) + m_s(5t^4 + 5w^4 + 3(x^2 + x(y - 1) + y(y - 1))(9x^2 + (y - 1)(9y - 21x \\
&- \quad 1)) + 2w^3(7x + 21y - z - 8) - 2z(x^2(18x - 43) - 62x - 9 - 17y + xy(31x + 58) + 2y^2(29 \\
&+ \quad 2x) - 32y^3) + z^2(10y(2 + 3y) - 53x^2 - 53 + 2x(56y - 79)) + 4z^3(13 + 16x - 6y) - 17z^4 \\
&+ \quad t^3(42x - 8w - 8(y + z - 1)) - t^2(3w^3 - 96x^2 - (7 + 19y - 25z - 52x)(y + z - 1) + 52wx \\
&+ \quad 2w(14z - 8y - 5)) + w^2(17 - 31x^2 - 116y + 20z + 12(8y - 3z)(y + z) + x(92z - 8y - 58)) \\
&+ \quad 2w(x^2(32 - 20y - 42z) - 18x^3 - x(y + z - 1)(37 + 29y - 71z) + (y + z - 1)(3 + 43y^2 + z \\
&\times \quad (21 - 23z) + y(20z - 49))) + 2t(43x^3 - 4w^3 + x(y + z - 1)(20 + 5y - 39z - 40x) - (29y \\
&- \quad 21z + 3)(y + z - 1)^2 + w^2(5 - 17x - 37y + 13z) - w(40x^2 + 2(y + z - 1)(1 + 31y - 19z) \\
&+ \quad x(12y + 56z - 37)))) + m_c\{t^4 - 10w^4 + 36x + 17x^2 - 52x^3 - x^4 + 36y - 47xy - 41x^2y \\
&+ \quad 52x^3y - 100y^2 - 14xy^2 + 24x^2y^2 + 92y^3 + 25xy^3 - 28y^4 + z(52x^3 - x(y - 1)(y - 123) \\
&+ \quad x^2(52y - 45) - 4(y - 1)(19y^2 - 20y - 3)) + z^2(32 + 28x^2 + x(138 - 77y) + 12y(3 - 5y)) \\
&- \quad z^3(51x + 4(7 + y)) + 8z^4 + t^2(y + z + w - 1)(6w + 84x + 4y + 8z - 3) - w^3(13x + 58y \\
&+ \quad 22z - 32) + 2t^3(8w + x + 8(y + z - 1)) + w^2(26x^2 + 156y + 36z - 6(y + z)(19y + z) - x \\
&\times \quad (y + 77z - 62)) + w(52x^3 + x(y + z - 1)(85 + 37y - 115z) + x^2(50y + 54z - 43) - 2(y + z \\
&- \quad 1)(6 + 47y^2 + z(5 - 7z) + y(40z - 61))) + t[5w^3 - 2x^3 + w^2(2 + 32x + 53y - 23z) + 120x^2 \\
&\times \quad (y + z - 1) + (y + z - 1)^2(12 + 43y - 33z) + 4x(y + z - 1)(7y + 9z - 5) + w(120x^2 + (y \\
&+ \quad z - 1)(19 + 91y - 61z) + x(60y + 68z - 52))]\}\Big)\Theta\Big[L_6[s, s', q^2, x, y, z, t, w]\Big]\Big]\Big\},
\end{aligned}
\tag{36}
$$

where

$$
\begin{aligned}
L_1[s, s', q^2, x, y, z, t] \quad &= \quad \frac{(x + y + z + t)}{\Lambda^2}\Big[(x + y + t - 1)\Big(- s'xt - sty - q^2xy + m_b^2y(x + t) \\
&+ \quad m_b^2y^2 + m_c^2x(x + y + t)\Big) + z(x + y + t - 1)(m_c^2x - s'x + m_b^2y - sy)
\end{aligned}
$$

$$
\begin{aligned}
&+ \quad z^2(m_c^2x - s'x + m_b^2y - sy) + m_s^2(t+z)\Lambda\Big],\\
L_2[s,s',q^2,x,y,z,t] &= \frac{(x+y+z+t)}{\Lambda^2}\Big[(x+y+t-1)\Big(- s'xt - sty - q^2xy + m_b^2y(x+t)\\
&+ \quad m_b^2y^2 + m_c^2x(x+y+t)\Big) + z(x+y+t-1)(m_c^2x + m_b^2(x+2y+t)\\
&- \quad st - q^2x) + z^2(m_c^2x - st - q^2x + m_b^2(x+2y+t-1)) + m_b^2z^3 + m_s^2t\Lambda\Big],\\
L_3[s,s',q^2,x,y,z,t] &= \frac{(x+y+z+t)}{\Lambda^2}\Big[(x+y+t-1)\Big(- s'xt - sty - q^2xy + m_b^2(x+y+t)\Big)\\
&- \quad z(x+y+t-1)(s't - ym_b^2 + yq^2) - z^2(s't - ym_b^2 + yq^2) + m_s^2t\Lambda\\
&+ \quad m_c^2(x+z)\Lambda\Big],\\
L_4[s,s',q^2,x,y,z,t,w] &= \frac{(x+y+z+t+w)}{\Lambda'^2}\Big[stx - st^2x + swx - stwx - sw^2x - stx^2 - swx^2\\
&- \quad m_c^2ty + s'ty + m_c^2t^2y - s't^2y - m_c^2wy + s'wy + twy(m_c^2 - s') + m_c^2w^2y\\
&- \quad s'w^2y - m_c^2xy + q^2xy + 2m_c^2txy - q^2txy - stxy - s'txy + m_c^2wxy\\
&- \quad swxy - s'wxy + m_c^2x^2y - q^2x^2y - m_c^2y^2 + 2m_c^2ty^2 - s'ty^2 + m_c^2wy^2\\
&- \quad s'wy^2 + 2m_c^2xy^2 - q^2xy^2 + m_c^2y^3 + z(-s'(t^2 + w(w+y-1) + t(x+y\\
&+ \quad w-1)) - x(sw + q^2(x+y+t+w-1)) + m_c^2(t^2 + w^2 + (x+2y)\\
&\times \quad (x+y-1) + w(x+3y-1) + t(2x+3y+w-1))) + z^2(-s'(t+w)\\
&- \quad q^2x + m_c^2(x+2y+2w+t-1)) + m_c^2z^3 + m_s^2(t+w)\Lambda' + m_b^2x\Lambda'\Big],\\
L_5[s,s',q^2,x,y,z,t,w] &= \frac{(x+y+z+t+w)}{\Lambda''^2}\Big[s'tw(1-t-w) - m_b^2tx + q^2tx + m_b^2t^2x - q^2t^2x\\
&- \quad m_b^2wx + swx + 2m_b^2twx - q^2twx - stwx + m_b^2w^2x - sw^2x - m_b^2x^2\\
&+ \quad m_b^2tx^2 - q^2txr + m_b^2wx^2 - swx^2 + m_b^2x^3 + s'wy - s'twy - s'w^2y\\
&- \quad m_b^2xy + q^2xy + m_b^2txy - q^2txy + m_b^2wxy - swxy - s'wxy + 2m_b^2x^2y\\
&- \quad q^2x^2y - s'wy^2 + m_b^2xy^2 - q^2xy^2 + \Big(q^2(y(1-y) - t(x+w+t-1)\\
&- \quad y(x+w+t)) - w(s(x+w+t-1) + s'(y+t)) + m_b^2z(t^2 + w^2 + (x\\
&+ \quad y-1)(2x+y) + w(3x+y-1) + t(3x+y+2w-1)) + z^2(m_b^2(2x\\
&+ \quad y + 2w + 2t - 1) - q^2(t+y) - sw) + m_b^2z^3 + m_s^2w\Lambda'' + m_c^2(y+t)\Lambda''\Big)\Big],\\
L_6[s,s',q^2,x,y,z,t,w] &= \frac{(x+y+z+t+w)}{\Lambda'''^2}\Big[s(-t^2(x+y) - t(x^2 + x(w+y-1) + y(w+y\\
&- \quad 1)) - w(x^2 + x(w+y-1) + y(w+y-1))) + z(-x(sw + q^2(x+w\\
&+ \quad t-1)) - y(s(t+w) + qr(x+w-1)) - q^2y^2 - s'(t^2 + w(w+y-1)\\
&+ \quad t(x+y+w-1)) + m_c^2(t^2 + w^2 + x(x-1) + y(x-1) + y^2 + t(2x\\
&+ \quad y + w - 1) + w(x+2y-1))) + z^2(m_c^2(x+2y+2w+t-1)\\
&- \quad q^2(x+y) - s'(t+w))m_c^2z^3 + m_s^2(t+w)\Lambda''' + m_b^2(x+y)\Lambda'''\Big], \qquad (37)
\end{aligned}
$$

and

$$\begin{aligned}
\Lambda &= t^2 - x - y - z(1-z) + (x+y)(x+y+z) + t(2x+2y+z-1), \\
\Lambda' &= t^2 + w^2 + z^2 + (x+y)(x+y+z) + t(2x+2y+z+w-1) + w(x+y+2z-1) \\
&- x - y - z, \\
\Lambda'' &= t^2 + w^2 + z^2 + (x+y)(x+y+z) + t(x+y+2z+2w-1) + w(x+y+2z-1) \\
&- x - y - z, \\
\Lambda''' &= t^2 + w^2 + z^2 + x^2 + y^2 + xy + z(x+2y-1) + t(2x+y+z+w-1) \\
&+ w(x+2y+2z-1) - x - y. \qquad (38)
\end{aligned}$$